

# The Dynamical Evolution of Triple Star Systems: A Numerical Study

E. Myles Standish, Jr.

Yale University Observatory

Received April 4, 1972

**Summary.** The initial conditions for 800 triple star systems are created and the evolution is followed, usually until the escape of one member. It is found that the angular momentum of the system is the quantity most influential in determining the following distributions: the time of disintegration, the velocity and mass

of the escaping particle, the semi-major axis, eccentricity and angular momentum of the remaining binary. These quantities are displayed graphically and discussed.

**Key words:** triple stars – three-body problem

## I. Introduction

This is a numerical study of the gravitational problem of three bodies. Eight different sets of initial conditions with 100 examples in each are selected to represent possible conditions at the birth of triple-star systems. The evolution is then followed numerically, and the results are analysed with respect to the probability and the average time of escape of one star, the mass and velocity of the escaper, and the semi-major axis, eccentricity and angular momentum of the remnant binary star system.

Previous numerical works of a similar nature include the following investigations: encounters of a binary by a passing star (Yabushita, 1966; Harrington, 1970); capture and binary formation from triple encounters (Agekyan *et al.*, 1970; Agekyan and Anosova, 1971); escape times (Agekyan and Anosova, 1967; 1968 and Anosova, 1969a, b); escape times and velocities of escapers (Worrall, 1967); and the effects of the mass distributions on many quantities (Szebehely, 1972). Also, Szebehely (1971) has classified the types of motion exhibited by three bodies in a plane.

This study advances the previous knowledge by analysing more quantities; in particular, ones more pertinent to astronomical questions. Furthermore, this study uses initial conditions which seem more realistic when the examples are related to triple star systems. In hindsight, it is seen that the inclusion of non-zero angular momentum is most significant.

Only two-dimensional motion is considered. It may be shown that if a three-body system has zero angular momentum, the motion of the system is confined to a plane. Since some of the examples computed in this study have zero angular momentum and are therefore two-dimensional, it was felt that the effect of non-zero angular momentum could best be observed by

confining all of the examples to a plane. Three-dimensional effects will be investigated in a later study. Section II introduces the notation used in this study, the choice of units and some relations between different parameters. Section III describes two features of the computer program. Section IV defines the different sets of initial conditions. Section V presents the numerical results. Section VI contains the conclusions.

## II. Choice of Units and Notation

The choice of units used in this study has been defined previously by the author (Standish, 1968). Briefly, the following equations hold for a cluster in equilibrium:

$$E = T + V,$$

$$2\hat{T} = -\hat{V},$$

$$\hat{T} = \frac{1}{2} M v_{\text{rms}}^2,$$

$$\hat{V} = -GM^2/2R^*,$$

$$t_{\text{cr}} = 2R^*/v_{\text{rms}},$$

where  $E$  is the total energy;  $T$ , the kinetic energy;  $V$ , the potential energy;  $M$ , the total mass;  $v_{\text{rms}}$ , the root-mean-squared velocity;  $G$ , the gravitational constant;  $R^*$ , a characteristic radius of the cluster; and  $t_{\text{cr}}$ , the crossing time.

The units of distance, mass and time are defined as  $R^* = 1$ ,  $M = 1$ , and  $t_{\text{cr}} = 1$ . This uniquely determines the rest:  $E = -2$ ,  $\hat{T} = 2$ ,  $\hat{V} = -4$ ,  $v_{\text{rms}} = 2$ , and  $G = 8$ .

With these units, the angular momentum of a lagrangian triangular equilibrium configuration is  $L^* = 0.777$ . The crossing time defined here is equal to 3 time units used by Agekyan and Anosova (1967).

The following formulae are useful for converting the present units into physical ones:

$$t_{\text{cr}} [\text{yrs}] = 0.45 \sqrt{R^{*3} [\text{A.U.}] / M [M_{\odot}]},$$

and

$$v_{\text{rms}} [\text{km/s}] = 21 \sqrt{M [M_{\odot}] / R^* [\text{A.U.}]},$$

remembering that  $v_{\text{rms}} = 2$  in the model units.

When the distance between two particles is much smaller than the distance of either to the third, the motion resembles two keplerian orbits. This motion occurs in Classes No. 2–4, proposed by Szebehely (1971). In all three cases (“Ejection without Escape”, “Escape”, and “Revolution”) the subscripts,  $3g$  and  $B$ , may be used to denote, respectively, the orbit of the remote body,  $m_3$ , relative to the center of mass of the remaining binary,  $m_a$  and  $m_b$ ; and the relative orbit of the binary itself.

For energy and angular momentum, the following relations hold:

$$E_{3g} = \frac{1}{2} \dot{\varrho}^2 - GM \left[ \frac{M_a}{\varrho_{3a}} + \frac{M_b}{\varrho_{3b}} \right] \approx \frac{1}{2} \dot{\varrho}^2 - GM/\varrho,$$

and

$$E_B = \frac{1}{2} \dot{r}^2 - G(m_a + m_b)/r;$$

$$h_{3g} = \varrho \times \dot{\varrho}, \quad \text{and} \quad h_B = r \times \dot{r};$$

where  $\varrho$  and  $r$  are illustrated in Fig. 1, and where  $M_a = m_a/(m_a + m_b)$  and  $M_b = m_b/(m_a + m_b)$ .

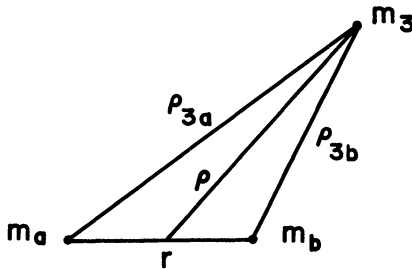


Fig. 1. The vector,  $\varrho$ , denotes the position of the remote body,  $m_3$ , with respect to the center of mass of the closer two,  $m_a$  and  $m_b$ .

For the system as a whole,

$$E = -2 = \frac{m_a m_b}{m_a + m_b} E_B + \frac{m_3(m_a + m_b)}{M} E_{3g},$$

and

$$L = \frac{m_a m_b}{m_a + m_b} h_B + \frac{m_3(m_a + m_b)}{M} h_{3g} = L_B + L_{3g}.$$

It may be seen that after escape ( $E_{3g} > 0$ ), the semi-major axis,  $a_B$ , and the angular momentum,  $h_B$ , are

bounded above by the relations

$$a_B \leq a^* = G \frac{m_a m_b}{2|E|}$$

$$\left\{ \begin{array}{l} = 2/9 \text{ when } m_a = m_b = 1/3 \\ \leq 1/2 \text{ when } m_a \neq m_b \end{array} \right\}$$

$$h_B^2 = G(m_a + m_b) a_B (1 - e_B^2) \leq G(m_a + m_b) a^* = h^*$$

$$\left\{ \begin{array}{l} = 32/27 \text{ for } m_a = m_b = 1/3 \\ \leq 4 \text{ for } m_a \neq m_b \end{array} \right\}.$$

### III. Computer Program

Once the initial conditions are specified, the equations of motion may be integrated numerically. The computer program used here takes advantage of a regularizing transformation developed by Peters (1968), whereby close encounters between two particles present no difficulties whatsoever.

A second feature of the computer program is the double-binary approximation. It often happens during the evolution of a three-body system that one of the particles nearly escapes (“Ejection without Escape”), traveling for a long time on an extended orbit, far away from the remaining pair. During this time, the motion of the third particle relative to the pair and the motion of the pair itself, both closely resemble keplerian orbits. Instead of integrating such motion numerically, the computer program approximates the motion with the aid of two-body formulae: the third body is advanced in its keplerian orbit to the point where it returns to the vicinity of the pair; the time for this advance is computed; and the binary pair is updated accordingly. Though such a method is admittedly an approximation to the true motion, it is felt that, statistically, it could not influence the results of the present study. Furthermore, the numerical integration of such a long stage of evolution would probably introduce more numerical error through round-off, etc., than that introduced by the double-binary approximation. The deciding factor is the enormous saving of computing time gained by use of the approximation. Even with the double-binary approximation, the change of the energy constant rarely exceeded 0.05%.

### IV. Initial Conditions

The different sets of initial conditions used in this study are denoted by a number and a letter. The letter, E or U, denotes equal or unequal masses, respectively. For the cases with unequal masses, three random numbers were generated and then normalized so that their sum,  $M$ , is equal to unity.

The initial positions were created, in all sets but the last (26U), by scattering three points at random inside a unit circle.

The center of mass for all cases is transferred to the origin. The initial conditions are always scaled so that the total energy is  $E = -2$ . This, with the choices of  $M = 1$  and  $G = 8$ , ensures the system of units described in Section II.

21 E, 21 U

Zero initial velocities for all three particles.

22 E, 22 U

"Rigid-body" rotation, about the center of mass, so that the angular momentum,  $L = L^*/3$ .

23 U

"Rigid-body" rotation such that the initial value of the virial ratio,  $2T_0/|V_0| = 1/2$ .

24 U

The closest pair of particles are given velocities so that they are in circular orbits about their common center of mass. The remote particle has zero initial velocity.

25 U

Random velocities, scaled and rotated so that, initially, the virial ratio,  $2T_0/|V_0| = 1$ , and the angular momentum,  $L = 0$ .

26 U

Each particle is placed at random inside a circle of radius 0.2, centered at the apex of an equilateral triangle of unit sides. The configuration is scaled and rotated so that  $2T_0/|V_0| = 1$ .

## V. Results of the Numerical Study

For each of the eight sets of initial conditions described above, 100 examples were computed and the evolution was followed until either 10000 integration steps had been taken or one of the particles had escaped. This latter event was determined when the conditions,  $q > 2.5$  and  $E_{3g} > 0$ , were fulfilled (i.e., hyperbolic ejection). Rigorous sufficient conditions for escape have been derived by the author (Standish, 1971), but these have not been used here since they were found after part of this study had been completed.

### Time of Escape

The time of escape,  $t_e$ , is defined here as the instant of time when the perimeter of the whole system attains its last local minimum before  $E_{3g}$  becomes positive. This time agrees in all cases with the time of pericenter passage of the escaper's hyperbolic orbit. However, the time of escape as defined, is not a true measure of how long all three bodies remain in proximity to each other. It often happens that "ejection without escape" occurs which lasts for an abnormally long time, during which one body remains widely separated. It becomes more meaningful, therefore, to define "nominal escape" as occurring when the condition,  $q > 10$ , is fulfilled. The associated "nominal escape time",  $t_e^*$ , is then a more realistic measure of the duration of "interplay" (Class No. 1 of Szebehely, 1971). This defini-

Table 1. Escape data

Set	Full escape		No escape		Nominal or Full escape
	$t_e < 1$	$t_e > 1$	Stable	Unstable	
21 E	5	94	0	1	99
21 U	18	82	0	0	100
22 E	4	95	0	1	100
22 U	8	89	1	2	99
23 U	15	59	26	0	78
24 U	13	87	0	0	100
25 U	26	70	0	4	100
26 U	4	93	0	3	99
Total	93	669	27	11	775

tion of nominal escape time is the same as that used by Agekyan and Anosova (1967, 1968).

Table 1 presents the general results of the numerical study. In 93 cases, the ejection of the escaping particle occurred immediately as a result of the initial conditions or as a result of the initial collapse of the system. In these cases,  $t_e < 1$ . In 669 cases, escape occurred after the evolution had shown some period(s) of "interplay" (usually short-lived), often separated by more extended periods of "ejection without escape". Of the 38 cases where escape never did occur, 13 had a nominal escape. 27 of the 38 cases showed motion which was judged (somewhat arbitrarily) to be stable. The other 11 showed unstable motion and it is likely that these cases would eventually lead to escape. The 38 cases roughly validate the finding by Harrington (1968) that a system is stable if one body remains widely separated from the other two (i.e.,  $q/r$  must be large). For this separation to remain large, the angular momentum,  $L$ , must also be large. Set 23 U is the only set of initial conditions likely to produce both such conditions.

The contributions of the different sets of initial conditions to the types of motion are evident from Table 1. In 682 cases, either full escape or nominal escape occurred after one crossing time ( $t_e > 1$ ). Figures 2a-h show histograms of these cases for the 8 sets of initial conditions. The mean value of  $t_e^*$  and the deviation of the mean ( $\sigma/\sqrt{n}$ ) are given in Table 2.

The initial conditions of set 21 E are the same type as those used by Agekyan and Anosova. The values of  $t_e^*$  agree well when the factor of 3 difference in units is applied:

$$\bar{t}_e^* (21 \text{ E}) \times 3 = 87.1 \pm 8.6,$$

$$\bar{t}_e^* (A + A) = 95.4 \pm 6.9.$$

### Mass of the Escaper

In order to illustrate the mass of the escaping particle, a scatter-diagram is presented in Fig. 3 for the 480 unequal-mass cases where full escape occurred after at least one crossing time. The mass of the escaper,  $m_3$ , is plotted on the horizontal axis. On the vertical axis is the mass of the smaller of the remaining two

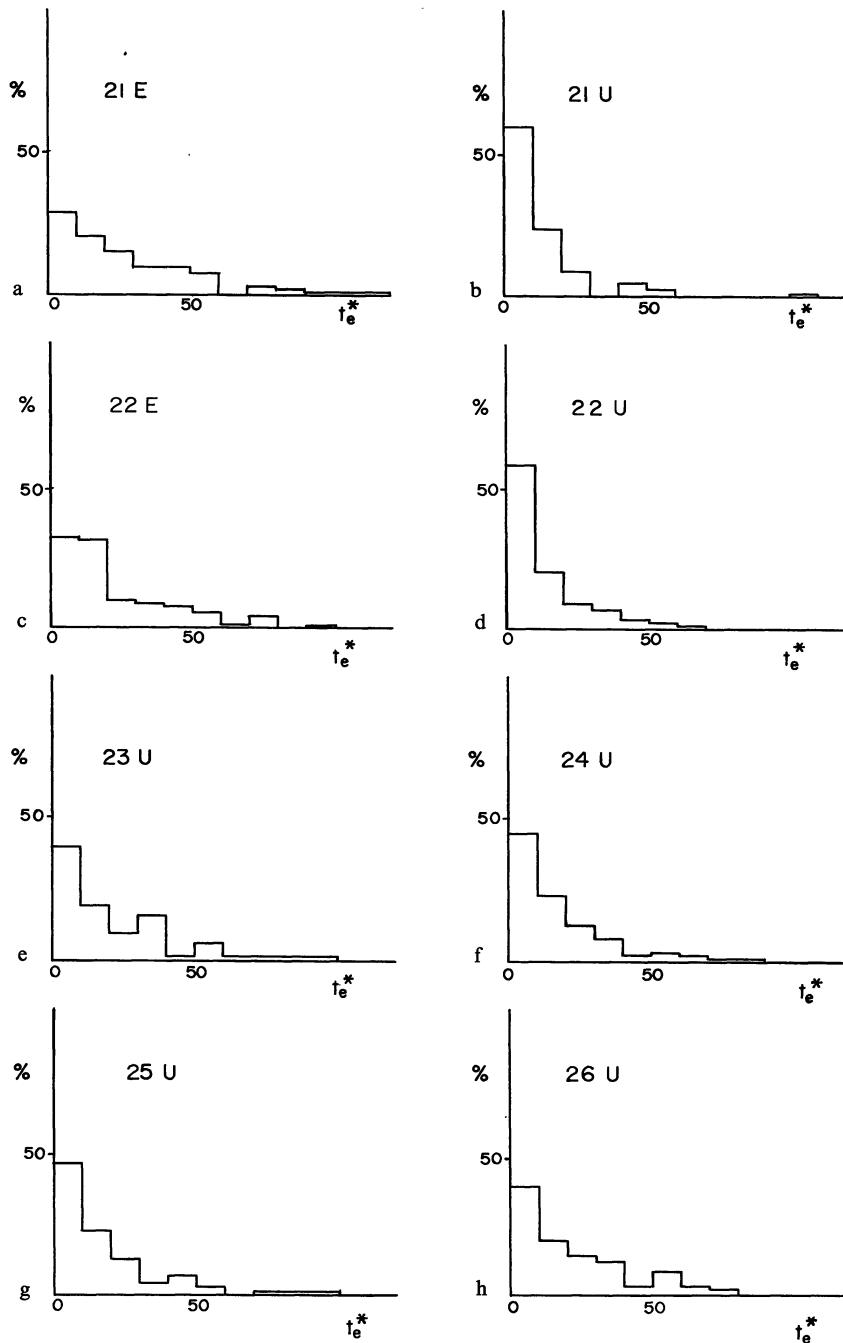


Fig. 2a-h. The distributions of the nominal escape times,  $t_e^*$ , for the systems where  $t_e^* > 1$ .

Table 2. Means and deviations. There were  $n$  cases of either full or nominal escape after one crossing time. There were  $m$  cases of full escape after one crossing time

SET	$n$	$t_e^*$	$m$	$e_B$	$a_B/a^*$	$h_B/h^*$	$L$
21 E	94	$29.03 \pm 2.85$	94	$0.742 \pm 024$	$0.697 \pm 024$	$0.466 \pm 027$	$0.000 \pm 000$
21 U	82	$13.10 \pm 1.83$	82	$901 \pm 018$	$768 \pm 022$	$258 \pm 024$	$000 \pm 000$
22 E	96	$24.60 \pm 2.58$	95	$851 \pm 016$	$725 \pm 021$	$362 \pm 023$	$256 \pm 000$
22 U	91	$18.63 \pm 5.53$	89	$806 \pm 022$	$774 \pm 021$	$413 \pm 026$	$256 \pm 000$
23 U	63	$25.75 \pm 4.75$	59	$593 \pm 029$	$905 \pm 012$	$713 \pm 024$	$545 \pm 017$
24 U	87	$18.62 \pm 2.17$	87	$769 \pm 029$	$792 \pm 021$	$437 \pm 030$	$247 \pm 014$
25 U	74	$26.10 \pm 5.32$	70	$829 \pm 025$	$741 \pm 028$	$362 \pm 031$	$000 \pm 000$
26 U	95	$25.51 \pm 4.11$	93	$553 \pm 029$	$933 \pm 006$	$734 \pm 021$	$627 \pm 015$

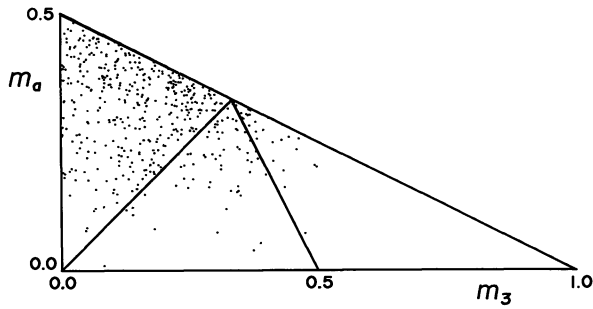


Fig. 3. The mass of the escaper is  $m_3$ . The smaller of the remaining two masses is  $m_a$

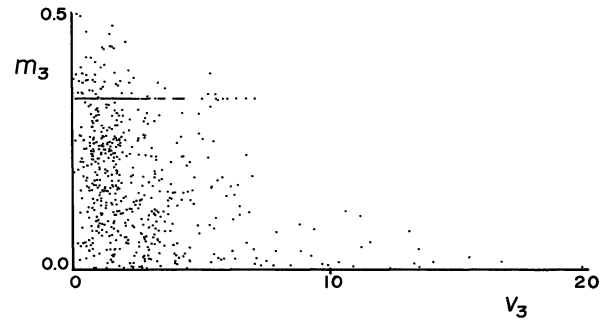


Fig. 4. The velocity of the escaper,  $v_3$ , versus its mass,  $m_3$ .

particles,  $m_a$ . The three sectioned areas correspond to the situations,

- $m_3 < m_a < m_b$  (385 members),
- $m_a < m_3 < m_b$  (66 members), and
- $m_a < m_b < m_3$  (29 members).

Points near to the upper (sloping line) indicate that  $m_a \cong m_b$ . Although the heaviest mass escaped in 29 cases, there was never a case where  $m_3 > 0.5$ .

#### Velocity of the Escaper

It is often asked whether the disruption of triple star systems can account for the presence of high-velocity "runaway" stars. Figure 4 is a scatter-diagram, plotting  $v_3$  vs.  $m_3$ , where  $v_3$  is the velocity of the escaper with respect to the center of mass of the whole system. Therefore,  $v_3$  would correspond to the space velocity of the escaping star. The values of  $v_3$  in km/s depend, of course, on the choices of  $M$  and  $R^*$ . For example, using the formula in Section II and choosing the values

$v_3 = 10$  ( $= 5 v_{\text{rms}}$ ),  $M = 30 M_\odot$ , and  $R^* = 100$  A.U., one finds a result of  $v_3 = 58$  km/s. This is a relatively high velocity for a star from a reasonable choice of units.

#### Eccentricity of the Binary

The distribution of the eccentricity of the remaining binary is illustrated in Figs. 5a–h by means of histograms. It is evident that the choice of equal masses tends to decrease the number of highly eccentric binaries at least for the cases of low angular momentum. More striking, however, is the effect of the initial amount of angular momentum in the system. As seen in Table 2, the sets 23 U and 26 U are the ones which have high angular momentum and consequently, less eccentric remnant binaries.

It is tempting to compare the distribution of eccentricity as found in this study with those derived from the observations of optical binary stars. Coureau (1960) finds a distribution function of the form,  $f(e) \sim (e - e^2)^{3/4}$ .

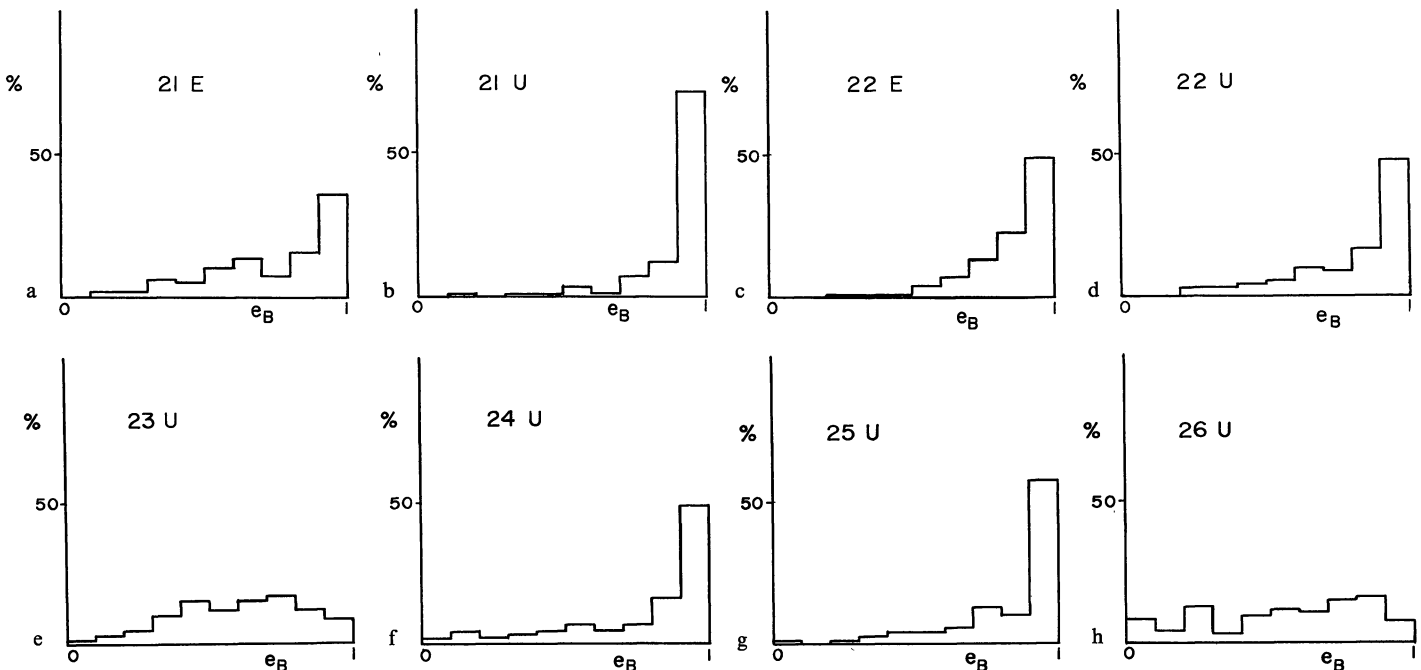


Fig. 5a–h. The distributions of the eccentricities of the remnant binaries after full escape has occurred

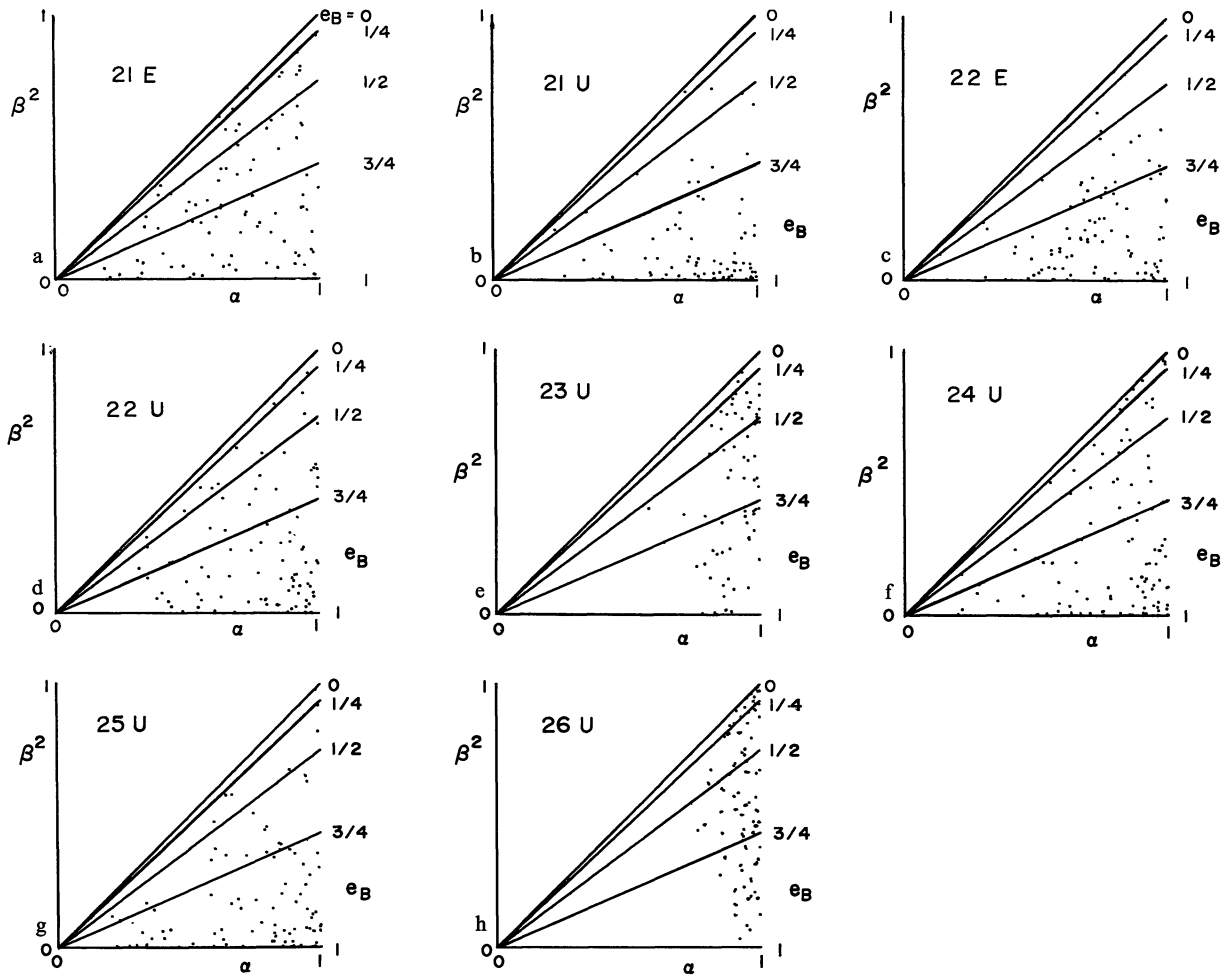


Fig. 6a-h. Scatter diagrams where  $\alpha = a_B/a^*$  and  $\beta = h_B/h^*$ , the ratios of the semi-major axes,  $a_B$ , and angular momenta,  $h_B$ , to their upper bounds,  $a^*$  and  $h^*$ , respectively. Lines of constant eccentricity,  $e_B$ , are drawn

To match such a function, the present study would indicate a high amount of angular momentum,  $L \approx \frac{3}{4} L^*$ . Caution is necessary on both sides, however. Selection effects would seem to exclude highly eccentric binaries from Couteau's data, while the point-mass approximation in the present study could tend to favor such cases. The comparison must therefore be taken lightly.

#### *Semi-major Axis, Angular Momentum*

The distribution of the semi-major axis,  $a_B$ , is relatively non-descript as such. Suffice it to say that it is rarely the case that  $a_B < 0.1$ . In other words, the dynamical disruption of triple stars does not produce tightly-bound binary stars.

More notable, however, are the distributions of the ratio,  $a_B/a^*$ , where  $a^*$  is the upper bound of  $a_B$  as discussed in Section II.

Similarly, for the angular momentum, the ratio of  $h_B/h^*$  is a more meaningful quantity than the value of  $h_B$  alone.

The distributions of  $a_B/a^*$  and of  $(h_B/h^*)^2$  may be inferred from Figs. 6a-h which are scatter-diagrams plotting these two quantities on the horizontal and vertical axes, respectively. The diagonal lines show the loci for equal values of the eccentricity,  $e_B$ , since

$$(h_B/h^*)^2 = (1 - e^2)(a_B/a^*).$$

It seems evident from the diagrams that the angular momentum of three-body systems is the major determining factor with respect to the description of the remnant binary. The difference between equal and unequal masses is also important but the effect is less clearly understood. For the cases with high angular momentum, the escaper is required to carry away a certain amount of angular momentum, since there is a bound on the amount which may be absorbed by the binary. In these cases, however, the binary tends to relieve the escaper by absorbing a relatively higher amount ( $h_B/h^*$  tends to be higher). In order to accomplish this, it must be the case that  $a_B/a^*$  is relatively large and that  $e_B$  is relatively small, as seen from the above equation.



## VI. Conclusions

The results of this paper may be summarized as follows:

- 1) Nearly all if not all triple star systems which contain some "interplay" during their evolution are dynamically unstable. The time of disruption may be delayed for a long time, however, by an "ejection without escape". The only systems known to be stable are the "revolution" cases.
  - 2) "Interplay" is short-lived. Ejection, with or without escape, usually occurs after only a few crossing times.
  - 3) The lightest mass usually escapes, though not always. The probability of a mass escaping which is heavier than the other two combined is extremely low, if not zero.
  - 4) High velocity escapers do occur, but they are usually the lighter mass stars.
  - 5) Tightly-bound remnant binaries are rare. The disruption of triple stars certainly can not account for spectroscopic binaries, unless extreme initial conditions are used.
  - 6) The distribution of eccentricity of the remnant binaries seems to be influenced most by the amount of angular momentum in the system. High angular momentum tends to produce less eccentric binaries.
  - 7) Angular momentum seems to be the most influential factor in the initial conditions.
- a) The Sundman inequality (see Pollard, p. 43),

$$L^2 \leq \sum m_i r_i^2 \sum m_i \dot{r}_i^2,$$

indicates in some fashion that the amount of sustained "interplay" is limited by the amount of angular momentum. This was seen in the present study. The "revolution" cases had high angular momentum; those with "interplay" had relatively little.

b) The different mechanisms for escape, not yet studied very closely, would seem to depend on certain ranges of angular momentum.

c) Since it is known that zero angular momentum implies two-dimensional motion, it seems likely that

small angular momentum would somehow limit the extent of motion out of the plane.

Further study of a similar nature would most profitably include a more systematic choice of initial conditions designed to illustrate specifically the effect of angular momentum. Inclusion of three-dimensional system would seem to be important also, since the third dimension is closely allied with the amount of angular momentum.

*Acknowledgements.* The author would like to thank Professor Victor G. Szebehely for providing valuable comments and discussions relating to this work.

This research was supported in part by a grant from the National Science Foundation to Yale University, NSF GP 26495; and in part by the Office of Naval Research under Contract, N 00014-67-A-0097-0018, NR 044-239.

## References

- Agekyan, T. A., Anosova, Zh. P. 1967, *Soviet Astr.* **11**, 1006.  
 Agekyan, T. A., Anosova, Zh. P. 1968, *Astrophysics* **4**, 11.  
 Agekyan, T. A., Anosova, Zh. P. *Soviet Astr.* **15**, 411.  
 Agekyan, T. A., Anosova, Zh. P., Bezgubova, B. N. 1970, *Astrophysics* **5**, 4.  
 Anosova, Zh. P. 1969a, *Astrophysics* **5**, 81.  
 Anosova, Zh. P. 1969b, *Publ. ast. Obs. Leningrad*, **26**, 88.  
 Couteau, P. 1960, *J. Observateurs, Marseille*, **43**, 41.  
 Harrington, R. S. 1968, *Astr. J.* **73**, 190.  
 Harrington, R. S. 1970, *Astr. J.* **75**, 1140.  
 Peters, C. F. 1968, Thesis, Yale Univ., New Haven.  
 Pollard, H. 1966, *Mathematical Introduction to Celestial Mechanics*. Prentice-Hall, Englewood Cliffs, N. J.  
 Standish, E. M. 1968, *Bull. Astr.* **3**, 3, 135.  
 Standish, E. M. 1971, *Cel. Mech.* **4**, 44.  
 Szebehely, V. G. 1971, *Cel. Mech.* **4**, 116.  
 Szebehely, V. G. 1972, preprint.  
 Worrall, G. 1967, *M.N.R.A.S.* **135**, 83.  
 Yabushita, S. 1966, *M.N.R.A.S.* **133**, 133.
- E. Myles Standish, Jr.  
 2023 Yale Station  
 New Haven, Conn. 06520, USA